JOURNAL OF AIRCRAFT
Vol. 41, No. 3, May–June 2004

Robust Structural Design of an Active Aeroelastic Wing with Maneuver Load Inaccuracies

P. Scott Zink,* Daniella E. Raveh,† and Dimitri N. Mavris‡
Georgia Institute of Technology, Atlanta, Georgia 30332-0150

A multidisciplinary design methodology for aircraft structures subject to inaccuracies in aerodynamic load predictions is presented. A statistical load-correction model is developed that is based on typical differences between loads as predicted by nonlinear and linear aerodynamic theories. Load corrections are propagated to a response function that represents the magnitude of structural redesign that would be necessary when the structure is subject to variation in the loads to which it was designed. The method is applied to an active aeroelastic wing concept, in which both the structural and control law designs are highly sensitive to variations in the aerodynamic loads. Computational fluid dynamics Euler analysis is used to construct the load-correction model. The most critical loading condition is then identified and used to redesign the structure and control-surface gear ratios. The redesigned structure was found to be 11% heavier and significantly more robust than the structure that was optimized with the linear loads only. The present methodology provides a way to account for load inaccuracies in the early phases of the design process, thereby, reducing the need for redesign late in the design process as load predictions become more accurate.

Introduction

THE structural design process typically relies on the use of low-fidelity, linear aerodynamic methods for the prediction of maneuver loads early in the design. These maneuver loads are not the actual flight loads. This results in a structure that is inadequate when subject to actual flight loads, often requiring significant redesign and increased weight. As a result, there is a motivation to acquire structural designs at the earliest phases of the design process that are robust to these inaccuracies, without imposing an unacceptable degree of conservatism. In this context, a robust structural design is one that is insensitive to inaccuracies in maneuver loads that are due to the use of linear aerodynamic theory for their prediction.

Furthermore, existing structural design methods are strained even further when new technologies are to be examined. Active aeroelastic wing (AAW) technology,[1] currently in a flight-test research program at the U.S. Air Force,[2] provides some unique challenges to the structural design of future fighter aircraft. AAW technology makes use of redundant wing control surfaces to provide maneuver load control and increased roll authority. It exploits the use of leading- and trailing-edge control surfaces to shape the wing aeroelastically, with the resulting aerodynamic forces from the flexible wing becoming the primary means for generating control power. With AAW, the control surfaces then act mainly as tabs and not as the primary sources of control power as they do with a conventional control approach. Wing flexibility is seen as an advantage rather than a detriment because the aircraft can be operated beyond control surface reversal speeds and still generate the required control power for maneuvers.

Presented as Paper 2002-5603 at the AIAA/ISMO 9th Symposium on Multidisciplinary Analysis and Optimization Atlanta, GA 4 September 2002; received 13 October 2002; revision received 12 November 2003; accepted for publication 12 November 2003.

*Ph.D. Candidate, School of Aerospace Engineering; currently Senior Aeronautical Engineer, Lockheed Martin Aeronautics Company, P.O. Box 748, Mail Zone 9382, Fort Worth, Texas, 76101. Member AIAA.

†Research Engineer II, School of Aerospace Engineering; currently Senior Lecturer, Faculty of Aerospace Engineering, Technion–Israel Institute of Technology, Haifa 32000, Israel. Member AIAA.

‡Boeing Professor of Advanced Aerospace Systems Analysis, School of Aerospace Engineering. Associate Fellow AIAA.

The AAW design process is defined as the concurrent optimization of the structure and control surface deflections or gear ratios. The control surface gear ratios dictate how one control surface deflects with respect to a single independent surface. Two gear ratio scenarios are shown in Fig. 1 in which the deflections of the leading-edge inboard (LEI), leading-edge outboard (LEO), and trailing-edge inboard (TEI) surfaces are linearly dependent on the deflection of the trailing-edge outboard surface (TEO). Historically, in the design of the gear ratios, more commonly known as trim optimization, the gear ratios are optimized to minimize an objective of stress, component loads, and/or control power.[3–7] The typical approach to the AAW design process, then, involves embedding trim optimization in an iterative process with structural optimization, to arrive at a simultaneously optimal control law and structure. In Ref. 7, such an AAW design process is presented in detail. In Ref. 8, a newly developed integrated approach is presented for the concurrent optimization of gear ratios and structural design variables, with the single objective of structural weight minimization. With the development of this deterministic process and the establishment of a wing structure and gear ratios optimized by the integrated AAW design process, as presented in Ref. 8, the current study focuses on a methodology for the design of the wing structure to be robust to maneuver load inaccuracies.

AAW design methods typically rely on linear aerodynamic theory for estimation of maneuver loads. Depending on the flight regime of interest, there may be significant discrepancies between the predicted loads and the actual loads acting on the aircraft. As a result, there is significant inaccuracy associated with maneuver loads estimated by linear aerodynamics. This inaccuracy could be alleviated by the use of wind-tunnel measured loads, or by the use of recently developed tools for computational-fluid-dynamics- (CFD-) based maneuver load analysis and structural optimization.[9,10] However, in consideration of a preliminary design study, in which multiple load evaluations are needed, neither wind-tunnel loads nor extensive use of CFD codes are practical. Thus, the retention of computationally inexpensive linear aerodynamic methods is desirable, as long as the structural design methodology accounts for the inherent inaccuracy associated with their use and provides ways to mitigate its effect. The present study presents a methodology to evaluate the effect of inaccuracies in the aerodynamic loads on a structural design employing AAW technology. In the current study, a CFD Euler analysis of the loads acting on the rigid configuration is used to define typical differences between linear and nonlinear wing loading. These differences are used to define the load corrections in a statistical manner. Then, for a given structural design, these corrections are propagated

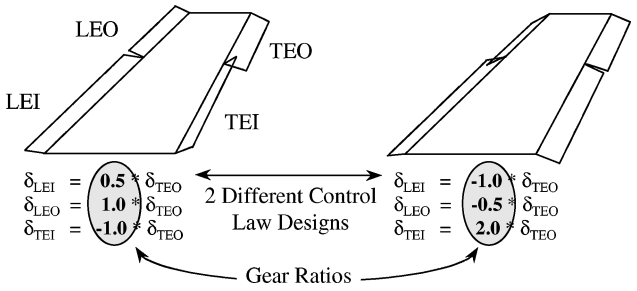

Fig. 1 Gear ratio.

to a response of interest to the structural designer. In the case of this study, the response of interest is a strain energy criterion that measures the amount of redesign that would be necessary should the loads change from their estimated values. The characteristics of this response are then used to redesign the structure to make it more robust to load variations.

Methodology

Introduction of Aerodynamic Load Corrections to the Aeroelastic Equations

The basic equation for the static aeroelastic analysis of a free aircraft by the finite element method in discrete coordinates is[11]

$$[[K] - q[AIC]]\{u\} + [M][\phi_R]\{\ddot{u}_R\} = [P]\{\delta\} \tag{1}$$

where $[K]$ is the stiffness matrix, the aerodynamic influence coefficients matrix $[AIC]$ is transformed to the structural degrees of freedom, $\{u\}$ are the displacements and rotations at the structural nodes, $[M]$ is the mass matrix, $[\phi_R]$ are the rigid-body modes of the free aircraft, $\{\ddot{u}_R\}$ is a vector of rigid-body accelerations, $[P]$ is a matrix of the rigid aerodynamic force coefficients due to aerodynamic trim parameters, q is the dynamic pressure, and $\{\delta\}$ is the vector of aerodynamic trim parameters, (for example, angle of attack, control surface deflections, pitch rate). The matrix $[P]$ contains columns corresponding to the rigid aerodynamic forces due to a unit deflection of each of the trim parameters, plus a column for each of the redundant control surfaces. A typical $[P]$ matrix for a symmetric maneuver of the AAW model would look like

$$[P] = [\{P\}_\alpha \quad \{P\}_{\mathrm{LEI}} \quad \{P\}_{\mathrm{LEO}}, \ldots, \{P\}_{\mathrm{TEO}}] \tag{2}$$

These forces are normally estimated by linear aerodynamic panel codes that are unable to capture nonlinear flow phenomena such as shocks and separated flow. As a result, there may be potentially large differences between the predicted rigid loads [the loads of Eq. (2)] and the actual nonlinear rigid loads acting on the aircraft, which may significantly affect the structural design. Hence, it is these vectors that are desired to be augmented with correction models. The load-correction models are based on typical differences between the aerodynamic loads as predicted by linear aerodynamic theory and the real nonlinear loads. The correction model does not assume the knowledge of the exact nonlinear loads acting at the trimmed flight condition. Rather, it is based on the knowledge of typical nonlinear aerodynamic attributes. It can be based, for example, on wind-tunnel testing performed on a similar configuration, or, as in the case of this study, on nonlinear aerodynamic loads from a CFD analysis.

Corrections to the rigid aerodynamic forces ($\{P\}_i$) are introduced to the static aeroelastic equation through the following formulation:

$$\{P\}_i = \{P\}_i^{\mathrm{lin}} + \eta_i\{\Delta P\}_i \tag{3}$$

where i refers to the aerodynamic trim parameter of interest, $\{P\}_i^{\mathrm{lin}}$ is the vector of rigid aerodynamic loads as predicted by linear aerodynamic theory, and $\{\Delta P\}_i$, herein referred to as correction load, is defined as

$$\{\Delta P\}_i = \{P\}_i^{\mathrm{nonlin}} - \{P\}_i^{\mathrm{lin}} \tag{4}$$

The vector $\{P\}_i^{\mathrm{nonlin}}$ refers to the rigid aerodynamic loads due to a unit deflection of trim parameter i, as computed by a CFD analysis. Because the purpose of introducing the correction loads is to capture nonlinear aerodynamic characteristics, which are not always evident at a deflection, or angle of attack, of 1 deg, $\{P\}_i^{\mathrm{nonlin}}$ may be evaluated for a larger deflection and then normalized by the deflection used to compute it. Although this linear scaling of nonlinear loads is invalid if accurate load distributions are required, it is justified by acknowledging that the role of $\{P\}_i^{\mathrm{nonlin}}$ is not to introduce accurate load estimation into the aeroelastic analysis, but rather to introduce a measure of how the nonlinear rigid load distribution may vary from the linear. It could be entirely possible that on the trimmed, flexible aircraft the linear loads may more closely represent the actual loads that the aircraft experiences. The reasons $\{P\}_i^{\mathrm{nonlin}}$ are not the true loads are several: 1) The high-fidelity models that are used to calculate $\{P\}_i^{\mathrm{nonlin}}$, such as Euler aerodynamics, are approximations, as well, and still can have an error associated with them. 2) $\{P\}_i^{\mathrm{nonlin}}$ is based on a rigid structure when in actuality the underlying structure is flexible, which has a large impact on the loads. 3) The nonlinear loads vary with the deflection of the trim parameters and cannot be simply scaled.

Because $\{P\}_i^{\mathrm{nonlin}}$ are not necessarily the true loads, and are a linear scaling of nonlinear aerodynamics, the significance of the contribution of $\{\Delta P\}_i$ to the linear rigid unit loads is related through a random variable η_i. The correction-load coefficients η_i are assigned probability distribution functions (PDFs) that are uniformly distributed between values of 0 and 1, where a value of 0 corresponds to the rigid unit loads as predicted by linear aerodynamic theory, that is, the rigid unit loads are $\{P\}_i^{\mathrm{lin}}$, and 1 corresponds to the rigid unit loads as predicted by nonlinear aerodynamic theory, that is, the rigid unit loads are $\{P\}_i^{\mathrm{nonlin}}$. The reason the PDF is defined to be uniform is due to the lack of knowledge and a priori statistical information of the loads actually acting on the aircraft. As a result, it is not desirable to favor one set of loads over the other (as would be the case if the distribution was skewed toward the nonlinear, that is, toward $\eta_i = 1$). However, there is no reason the correction-load coefficient range cannot be larger. In fact, making it larger increases the range of possible loading conditions and might lend more confidence that the structure designed to these loads is more robust. This exploration is left for future studies.

For an AAW, a gearing matrix $[G]$ relates the deflections of the dependent control surfaces to the independent trim parameters $\{\delta_I\}$ (Ref. 7) . The right-hand side (RHS) of the discrete static aeroelastic equation of motion [Eq. (1)], with the introduction of the gearing matrix, is defined as

$$\mathrm{RHS} = [P][G]\{\delta_I\} \tag{5}$$

With the introduction of the load correction model, Eq. (5) becomes

$$\mathrm{RHS} = [P]^{\mathrm{lin}}[G]\{\delta_I\} + [P]^{\mathrm{corr}}[G]\{\delta_I\} \tag{6}$$

where $[P]^{\mathrm{lin}}$ are the original, linear rigid aerodynamic unit loads and

$$[P]^{\mathrm{corr}} = [\eta_\alpha\{\Delta P\}_\alpha \quad \eta_{\mathrm{LEI}}\{\Delta P\}_{\mathrm{LEI}}, \ldots, \eta_{\mathrm{TEO}}\{\Delta P\}_{\mathrm{TEO}}] \tag{7}$$

In this study, modal-based analysis and optimization are being employed.[12,13] It is assumed that the discrete displacements $\{u\}$ of Eq. (1) can be represented by a linear combination of the modes of vibration of the free aircraft as given by

$$\{u\} = [\phi_R \quad \phi_E]\begin{Bmatrix}\xi_R\\ \xi_E\end{Bmatrix} \tag{8}$$

where $[\phi_R \ \phi_E]$ is the modal matrix comprising the rigid-body modes $[\phi_R]$ of the free aircraft, and a subset of the elastic modes $[\phi_E]$. Here $\{\xi_R\}$ are the rigid-body displacements, and $\{\xi_E\}$ are the elastic modal displacements. Substituting the modal assumption of Eq. (8) into Eq. (1), and pre-multiplication by the transpose of the modal matrix, yields the AAW aeroelastic equation of motion in

modal coordinates,

$$\begin{bmatrix} -qGAIC_{RR} & -qGAIC_{RE} \\ -qGAIC_{ER} & GK_{EE} - qGAIC_{EE} \end{bmatrix} \begin{Bmatrix} \xi_R \\ \xi_E \end{Bmatrix} + \begin{bmatrix} M_{RR} \\ M_{ER} \end{bmatrix} \{\ddot{\xi}_R\} = \text{RHS}^{\text{modal}} \tag{9}$$

where

$$[GK_{EE}] = [\phi_E]^T [K][\phi_E]$$

$$[M_{RR}] = [\phi_R]^T [M][\phi_R] \quad [M_{ER}] = [\phi_E]^T [M][\phi_R]$$

$$[GAIC_{RR}] = [\phi_R]^T [AIC][\phi_R] \, [GAIC_{ER}] = [\phi_E]^T [AIC][\phi_R]$$

$$[GAIC_{RE}] = [\phi_R]^T [AIC][\phi_E] \, [GAIC_{EE}] = [\phi_E]^T [AIC][\phi_E] \tag{10}$$

and using the RHS of Eq. (6),

$$\text{RHS}^{\text{modal}} = [\phi_R \quad \phi_E]^T \left([P]^{\text{lin}} [G]\{\delta_I\} + [P]^{\text{corr}} [G]\{\delta_I\} \right) \tag{11}$$

The modal aeroelastic equation (9) is solved together with Eq. (12), which states that, for a free aircraft, the displacements do not change the location of the center of gravity with respect to the mean axis system, nor the orientation of the mean axis system,[14]

$$[\phi_R]^T [M][\phi_R \quad \phi_E] \begin{Bmatrix} \xi_R \\ \xi_E \end{Bmatrix} = \{0\} \tag{12}$$

Solving Eq. (12) for the rigid-body modal displacements and substituting it into Eq. (9) yields

$$\begin{bmatrix} q[GAIC_{RR}][M_{RR}]^{-1}[M_{ER}]^T - q[GAIC_{RE}] \\ q[GAIC_{ER}][M_{RR}]^{-1}[M_{ER}]^T + [GK_{EE}] - q[GAIC_{EE}] \end{bmatrix} \{\xi_E\} + \begin{bmatrix} M_{RR} \\ M_{ER} \end{bmatrix} \{\ddot{\xi}_R\} = \text{RHS}^{\text{modal}} \tag{13}$$

Solving the second row of Eq. (13) for $\{\xi_E\}$, and substituting the resulting $\{\xi_E\}$ into the first row of Eq. (13), yields the aeroelastic trim equation,

$$[L]\{\ddot{\xi}_R\} = [R][G]\{\delta_I\} \tag{14}$$

where

$$[L] = [M_{RR}] + q[GAIB_{RE}][GKA_{EE}]^{-1}[M_{ER}] \tag{15}$$

$$[R] = \left([\phi_R]^T [P]^{\text{lin}} + [\phi_R]^T [P]^{\text{corr}} \right) + q[GAIB_{RE}][GKA_{EE}]^{-1} \left([\phi_E]^T [P]^{\text{lin}} + [\phi_E]^T [P]^{\text{corr}} \right) \tag{16}$$

$$[GAIB_{RE}] = [GAIC_{RE}] - [GAIC_{RR}][M_{RR}]^{-1}[M_{ER}]^T \tag{17}$$

$$[GKA_{EE}] = q[GAIC_{ER}][M_{RR}]^{-1}[M_{ER}]^T + [GK_{EE}] - q[GAIC_{EE}] \tag{18}$$

Equation (14), through $[R]$, is characterized by a term due to linear-only aerodynamics and an additive correction term that attempts to quantify the possible variation in the generalized rigid aerodynamic loads. As a result of introducing correction to only the RHS of the aeroelastic equation, the CPU-intensive decomposition of the left hand side does not have to be repeated every time the correction-load coefficients change. This is especially beneficial because statistical methods, particularly sampling methods, require many function evaluations to generate a cumulative distribution function (CDF) of a system response. This allows for application of more accurate statistical methods, such as Latin hypercube sampling (LHS).[15]

Robust Structural Design with Maneuver Load Corrections

In the Introduction, a robust structural design was defined as one that is insensitive to inaccuracies in maneuver loads, or in other words, one that would not require significant redesign as loads predictions become more accurate. With the preceding formulation of the static aeroelastic equation with load corrections, a possible way to find a robust structural design would be to use a reliability-based optimization (RBO)[16,17] approach, in which the structural design variables and the gear ratios are optimized to minimize weight and meet the static aeroelastic constraints of the maneuvers for a desired probability level. However, in consideration that several maneuvers could be examined, with thousands of constraints per maneuver, the RBO approach would be far too computationally burdensome for a realistic preliminary structural design problem. Another possible, straightforward approach for finding a robust design would be to optimize the structure to every possible loading condition that results from variation in the correction-load coefficients. For each sample of the correction-load coefficient design space, then, this would result in an additional maneuver in the AAW design process for the structure and gear ratios to be designed to. If one was to examine many of these samples in an effort to cover the design space, one could easily imagine hundreds of additional maneuvers in the optimization. This again, is a computationally, cost-prohibitive approach.

As a result, an alternative approach for finding a robust structural design is developed. The latter approach, just discussed, would have merit if a small number of cases could be identified that are most critical and the structure designed to these. In this way, then, the subsequent optimization would be much more manageable and more useful in the preliminary design phase, where many maneuvers are examined, and many details of the design are not fixed. The general philosophy of this approach is outlined.

The first phase of the robust design process, presented here, is an integrated AAW design that results in optimal structural element thickness and gear ratios, for a set of maneuvers, based on linear aerodynamics.[8] The second phase involves analyzing this structure and control law on its ability to maintain strength requirements in the presence of maneuver-load corrections as defined in the preceding section. Sampling methods are used to propagate the load corrections to a criticality criterion, from which a CDF of this criterion is generated and a point in the correction-load coefficient design space that is most critical is identified. The criticality criterion is reflective of how much the structure would need to be redesigned if the loads were to change from their originally estimated values. In the final phase, the structure and gear ratios are redesigned to this most critical case. The resulting structure should be more robust than the one based on linear aerodynamics only, meaning that the analysis of the redesigned structure in the presence of maneuver load correction should result in a small (or zero) criticality criterion value with little (or no) variation.

The methodology assumes that, with the application of more realistic loads, the gear ratios can change, to optimize them for the actual loading condition, but that the structure is fixed. Because it is far cheaper to change the gear ratios than it is to change the structure, it is a robust structure rather than a robust control law that is desired.

The approach here of designing to the most critical case is justified for the following reasons: 1) Traditional robust design techniques with separation of variables into noise and control variables and then selection of the control variables to minimize variance of the response (or maximize probability of achieving a target) is difficult in a complex structural design process where the number of design variables is large (in this case 78) and the number of constraints even larger (in this case 3808 per maneuver). 2) In a preliminary design setting, it is usually desirable to take more weight early in the design process rather than to have to add some later. As a result, a conservative design early in the process is not as detrimental. It is typically easier to take off weight than it is to add it.

Development of Strain Energy Criterion

With the introduction of load corrections to the linear loads, a means of determining what values of correction-load coefficients

are the most critical to the structure is necessary. Essentially, one desires to know what values of the coefficients would result in the most significant redesign of the wing. For the purposes of the research here, this means the largest increase in weight that would be necessary to make the structure meet the design constraints when subject to the new loads.

Because the primary constraints of the integrated AAW design process are strain constraints, a potential criterion would be based on the violated strain constraints when the structure is analyzed with the perturbed loads. (Perturbed loads here refer to the linear rigid unit loads plus a contribution from the correction loads.) The conditions leading to the formulation of the strain criterion were as follows.

1) The criterion should reflect the size of the elements. For example, if an element of a large area and an element with a small area have the same positive (violated) strain constraint value, the larger area element will require more material to make the constraint feasible than the smaller one. A good basis for this criterion is the element strain energy because, for the same level of strain, the larger the element the larger the strain energy.

2) The criterion, when evaluated for the perturbed loads, should be compared to a reference case that is based on the original loads to which the structure was designed.

3) Only the strain energy of elements that are designed and whose constraints are violated should be considered.

Based on the preceding conditions, a strain energy criterion is defined as the difference in element strain energy only for those elements whose constraints are violated in the perturbed case:

$$Cr = \sum_{j=1}^{n_{\text{el}}} \left(U_j^{\text{perturbed}} - U_j^{\text{reference}}\right) \cdot I\left(g_j^{\text{strain}} > 0\right)$$

$$I = \begin{cases} 1 & g_{2j-1}^{\text{strain}} > 0 \quad \text{or} \quad g_{2j}^{\text{strain}} > 0 \\ 0 & \text{otherwise} \end{cases} \tag{19}$$

where n_{el} refers to the number of designed elements. $U_j^{\text{perturbed}}$ is the strain energy of the jth element for the perturbed case. $U_j^{\text{reference}}$ is the strain energy of the jth element when subject to the linear-only rigid loads. Here g_j^{strain} is the strain constraint for the jth element, where a positive g_j^{strain} value reflects a violated constraint. The reason there are two constraint conditions for each element is that there are two constraints per element: 1) a fiber strain constraint and 2) a transverse strain constraint. Hence, if either one of these constraints is violated for an element, the strain energy difference between the perturbed and reference case is accounted for.

Numerical Example

Structural and Linear Aerodynamics Models

Figure 2 shows the structural model used both in Refs. 7 and 8 and in the current study. It is a preliminary-design finite element model of a lightweight fighter composite aircraft with four wing control surfaces (two trailing edge) and two leading edge) and a horizontal tail.[12] The skins of the wing are made up of four composite orientations, 0-, ±45-, and 90-deg plies, where the thickness of the −45- and +45-deg orientations are constrained to be equal. The structural design variables for the optimization are the layer thickness of the composite skins. The number of structural design variables is 78 due to physical linking of the skin elements. Internal structure and carry-through structure are fixed.

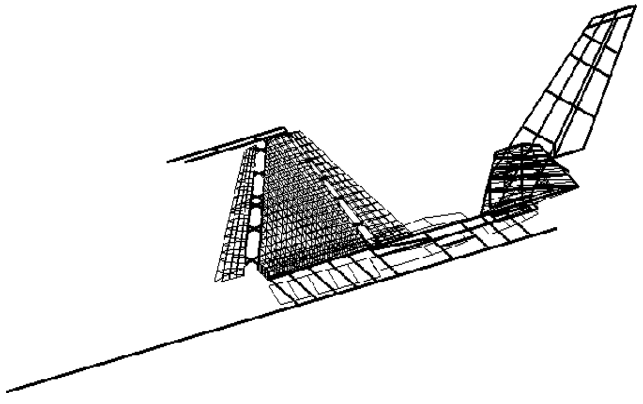

Fig. 2 Structural model.

Table 1 Maneuver conditions and design constraints

Maneuver condition	Design constraint, fiber strain
1) Mach 0.95, 10,000 ft, 9 g pull up	3000 $\mu\varepsilon$ tension 2800 $\mu\varepsilon$ compression
2) Mach 1.20, sea level, 3 g push over	3000 $\mu\varepsilon$ tension 2800 $\mu\varepsilon$ compression
3) Mach 1.20, sea level, steady-state roll 100 deg/s	1000 $\mu\varepsilon$ tension 900 $\mu\varepsilon$ compression
4) Mach 0.95, 10,000 ft, steady-state roll 180 deg/s	1000 $\mu\varepsilon$ tension 900 $\mu\varepsilon$ compression

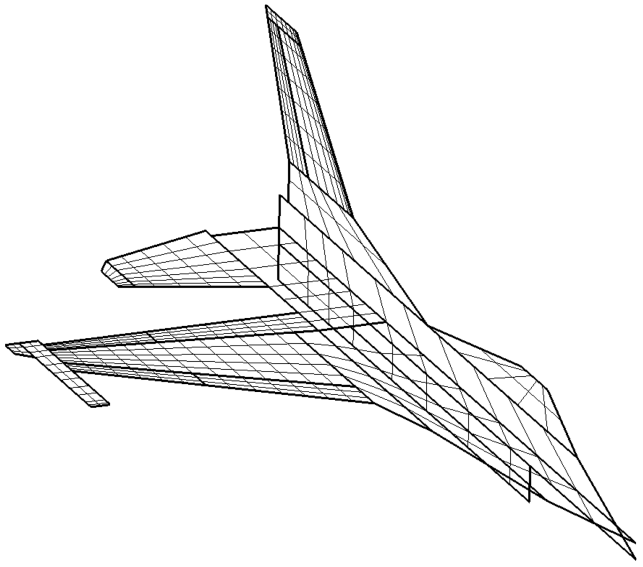

Fig. 3 Linear aerodynamic model.

The linear aerodynamic model, from which the linear force coefficients $\{P\}^{\text{lin}}$ are estimated, is shown in Fig. 3. It is a flat panel Carmichael model[18] containing 143 vertical panels and 262 horizontal panels. It also contains paneling for the four wing control surfaces and horizontal tail to coincide with the control surfaces on the structural model. Carmichael aerodynamic influence coefficients are produced for two Mach numbers, 0.95 and 1.2, for both symmetric and antisymmetric maneuvers (see Ref. 19).

Table 1 presents the maneuver conditions and strength constraints to which the structure is designed (where $\mu\varepsilon$ is micro-strain and g is load factor). In addition to the strength constraints, hinge moment constraints and control surface travel limits are also included.

For each maneuver, the deflections of 4 of the 5 control surfaces are linked to the remaining surface (or independent surface) via the gear ratios. The horizontal tail was selected as the independent surface for maneuvers 1 and because it has historically been the primary control surface for symmetric trim. The LEO surface was selected for maneuver 3, because it is the most effective surface at supersonic conditions. For maneuver 4, the TEO surface was chosen because it is the most effective roll control surface at subsonic speeds.

The gear ratios for each maneuver and the structural design variables were optimized for the maneuver constraints, by use of the integrated AAW design process in Ref. 8, which employed linear aerodynamics. The current paper presents the results of the proposed robust design methodology on the optimal structural design and gear ratios of the integrated AAW design process. However, in

this study maneuver load correction has only been introduced to the Mach 0.95 subsonic, pull up.

Nonlinear Aerodynamics Model

The surface grid of the nonlinear aerodynamic model is shown in Fig. 4. The flowfield around the wing and fuselage was evaluated using an H-type grid, with four grid zones representing the upper and lower wing and its wake and the upper and lower fuselage and its wake.

The flow was analyzed by the CFL3D[20] Euler/Navier–Stokes code using its Euler option for various Mach numbers and angles of attack. Figure 5 shows the pressure distribution at $\alpha = 1$ deg and Mach 0.95, where shocks on the upper and lower surface are observed. It was decided to use the flowfield corresponding to $\alpha = 1$ deg as a characteristic nonlinear load distribution for the generation of the correction load for angle of attack.

The nonlinear forces acting on the wing surface were splined to the linear aerodynamic model nodes using the spline technique in Ref. 10, which is based on the infinite plate spline method.[21] These loads then served as $\{P\}_i^{\text{nonlin}}$ in the correction load calculation of Eq. (4) and were used to model the load correction due to a unit angle of attack. For the nonlinear force vector due to a unit deflection of each control surface, the flow analysis was repeated for the same flight condition at $\alpha = 0$ deg with the control surface deflected to 1 deg. The current CFD model (Fig. 4) does not have a horizontal tail, and therefore, corrections to the horizontal tail aerodynamics were not considered in this study. Typically, in the presence of a tail there is significant interaction between the lift surfaces, which greatly affects the loads, and this interaction is not captured in the current load-correction model. However, as discussed in the methodology section, the current study is not focused on linear vs nonlinear comparisons but rather presents a method for accounting for loads that differ from those predicted by linear aerodynamics. In this study the tailless configuration nonlinear loads serve as a loading case that differs from the linear loading case.

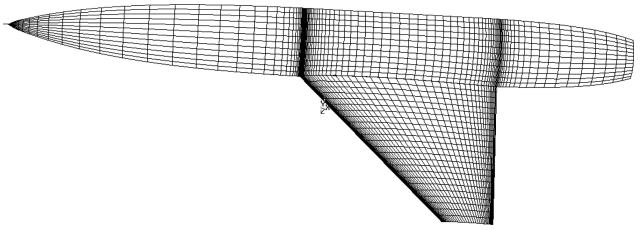

Fig. 4 Nonlinear aerodynamic model.

Aeroelastic Analysis with Correction Loads

LHS was used to sample from the correction-load coefficient design space, and then for each sample, static aeroelastic analysis using modal-based ASTROS was performed to evaluate the strain energy criterion. The results of this analysis were then to determine the correction-load coefficients that resulted in the highest strain energy criterion and also to obtain an estimate of the variation in the criterion due to corrections.

The case presented next demonstrates how the gearing ratios can be grossly inadequate when the actual flight loads differ from the predicted load, that were for used for gear ratio optimization, and how the introduction of correction loads will identify this problem and provide a solution to it.

Aeroelastic analysis revealed that introduction of the correction load for the TEI surface resulted in very large strain energy criterion values and a massive number of violated constraints. On further investigation, when only the TEI correction load across a range of values for η_{TEI} between 0 and 1 was examined (with $\eta_\alpha = \eta_{\text{LEO}} = \eta_{\text{LEI}} = \eta_{\text{TEO}} = 0$), an asymptotic behavior was discovered. This is shown in Fig. 6, which is the strain energy criterion vs η_{TEI}. The deflections of the independent trim parameters, that is, horizontal tail deflection and angle of attack, as a function of η_{TEI} are also plotted against the secondary axis, in Fig. 6.

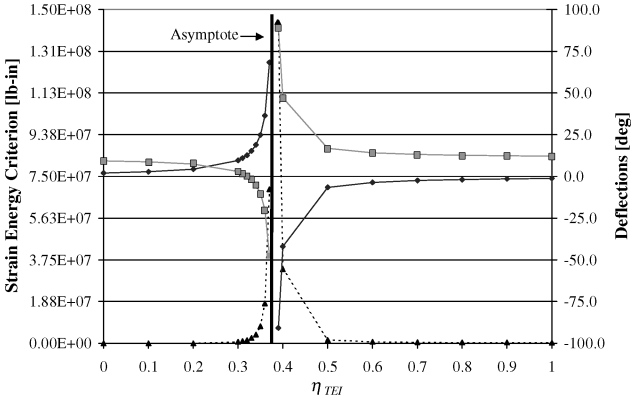

Fig. 6 Strain energy criterion and independent trim parameters vs η_{TEI} (fixed gear ratios): ▲, criterion; ♦, horizontal tail; and ■, angle of attack.

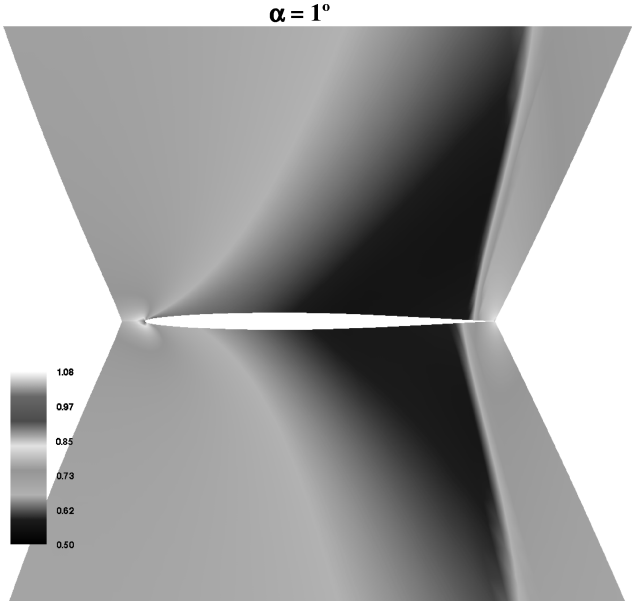

Fig. 5 Pressure distributions of wing cross section (Mach 0.95, 51% semispan).

Table 2 Gear ratios of subsonic pull up in load-correction analysis

Control surface	Gear ratio
g_{LEI}	−5.64
g_{LEO}	−14.67
g_{TEI}	14.60
g_{TEO}	−14.67

Table 3 Fixed deflections of the control surfaces

Control surface	Deflection, deg
δ_{LEI}	−11.52
δ_{LEO}	−30.00
δ_{TEI}	29.86
δ_{TEO}	−30.00

The asymptotic behavior of the trimmed deflections of the horizontal tail and angle of attack indicate that $[R][G]$ in the RHS of the trim equation (14) is becoming singular as η_{TEI} nears a value of 0.38 because solution of the trimmed deflections $\{\delta_I\}$ requires inversion of this matrix. For the subsonic pull-up maneuver, $[R][G]$ of Eq. (14) is a 2×2 matrix corresponding to aeroelastic lift and pitching moment due to angle of attack and the horizontal tail. In the analyses that led to this phenomenon, the wing control surfaces were geared to the horizontal tail according to the optimal gear ratio values that were found in the integrated AAW design process.[8] These gear ratios are presented in Table 2.

At $\eta_{\text{TEI}} = 0$, the horizontal tail and angle of attack are deflecting to their final values as found by the integrated AAW design process with linear aerodynamics. These values are $\alpha = 9.31$ deg and $\delta_{\text{HT}} = 2.05$ deg. In this case the horizontal tail, with the wing control surfaces geared to it, provides positive lift and pitching moment (nose up) with a positive horizontal-tail deflection. This accounts for the positive, non-traditional deflection of the horizontal tail. The introduction of nonlinear loads for the TEI surface, while keeping the gear ratios unchanged, produces negative pitching moment. As η_{TEI} gets larger, the horizontal tail deflects more positively to counteract the negative pitching moment from the nonlinear loads. The positive deflection of the horizontal tail increases lift; hence, the angle of attack is decreased, up to a point at which the angle of attack actually becomes negative (near $\eta_{\text{TEI}} = 0.32$). This rather absurd trend continues to the asymptote at a value of 0.381, at which point $[R][G]$ becomes singular. Above this value the trend reverses, with the horizontal tail deflecting negatively and angle of attack being positive.

This phenomenon demonstrates that keeping the gear ratios fixed while introducing load variations might be totally inadequate and severely detrimental. For the case of the subsonic pull up, the AAW design using linear loads ended with a control law in which the horizontal tail was deflected slightly positively, which contributed to the total lift, whereas the pitching moment balance was achieved through the use of the wing control surfaces. Although this control law seems to be better than a traditional one (in which the horizontal tail deflects negatively, subtracting from total lift), the introduction of load variations revealed that this control law is not robust and may be catastrophic under certain possible loading conditions. The identification of such phenomena, which is crucial for the design of the control law and structure, was made possible only with the introduction of the load-correction models and analysis.

Fixed Control Surface Deflections Approach

Ideally, the gear ratios should be redesigned, that is, optimized, each time the correction-load coefficients change, to minimize the element strains or strain energy criterion. However, at present, such a tool is not directly available. A solution to the problem has been to fix the deflections of the wing control surfaces to their optimized values as opposed to fixing their gear ratios. In this way, the horizontal tail is freed from the wing control surfaces and allowed to be the independent surface, by itself. The optimal control surface deflections by the AAW design process with linear aerodynamics are presented in Table 3.

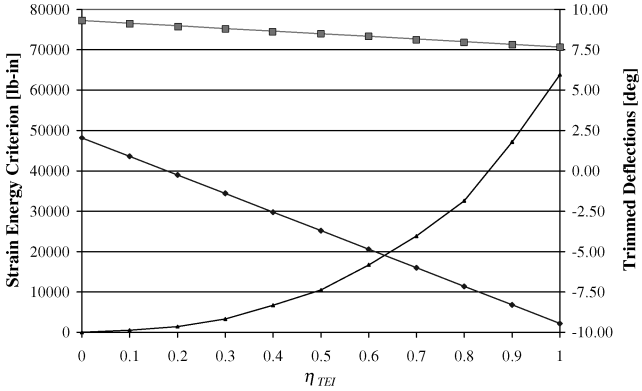

Fig. 7 Strain energy criterion and independent trim parameters vs η_{TEI} (fixed deflections): ▲, criterion; ♦, horizontal tail; and ■, angle of attack.

Figure 7 shows the variation of the strain energy criterion and the trimmed angle of attack and horizontal tail deflection vs η_{TEI} when the wing surfaces have fixed deflections. When compared with Fig. 6, one notices dramatic differences between fixing the gear ratios and fixing the deflections. The horizontal tail deflection switches in sign from positive to negative with increasing contribution from the nonlinear loads. This is understandable because introduction of nonlinear loads for the TEI surface causes more pitch-down moment (due to backward shift of the center of pressure), and thus the horizontal tail must begin to act in its traditional role (deflecting negatively) to provide positive pitch-up moment.

It is likely that the real loads acting on the tailed configuration are somewhat different than the loads used here, which were computed for a tailless configuration. However, the trend of shifting the center of pressure backward is correct and typical of nonlinear flows in the presence of a shock wave. Thus, the case of inadequate gear ratios, as was presented in the last section, is realistic and likely to occur when the aircraft is subject to the real flight loads.

The correction loads for the other control surfaces have also been introduced into the analysis, using the earlier described fixed deflection approach, and their individual impacts on the strain energy criterion have been examined. Similar to the preceding case of the TEI control surface, the strain energy criterion increases smoothly with increasing values of each of the other correction-load coefficients, although the magnitude of the criterion as a function of each coefficient is not nearly as high as in the case of Fig. 7. Hence, it is the variation in the TEI surface that turns out to have the largest impact on the strain energy criterion.

Although introduction of each correction load by itself causes an increase in the strain energy criterion, it was found that when other correction-load coefficients are non-zero an increase in the correction-load coefficient for the TEO surface actually acts to relieve the strain energy criterion. This suggests that there is a heavy interaction between the TEO loads and the others. This point is shown in Fig. 8, which is the strain energy criterion vs η_{TEI} and η_{TEO}, while the other correction-load coefficients are zero.

Note that the point with the largest criterion value occurs at a value of $\eta_{\text{TEI}} = 1$ and $\eta_{\text{TEO}} = 0$, and that no point in the interior of the design space is more critical, that is, has a higher strain energy criterion value, than this point. The observation from both Figs. 7 and 8 indicate that the most critical point is on the corner of the correction-load coefficient design space. The dimension of this design space is 5, resulting in 2^5 (or 32) corners points. Table 4 shows a number of these corner points where each correction-load coefficient ranges between 0 and 1. The strain energy criterion for the original structure, designed with linear aerodynamics only, is presented in the seventh column of Table 4. The case with the highest criterion value is case 31.

To confirm that indeed the most critical point lies on a corner of the design space and also to obtain an estimate of the amount of variation

Table 4 Strain energy criterion for linear-only and redesigned structures

Case	η_α	η_{LEI}	η_{LEO}	η_{TEI}	η_{TEO}	Criterion, lb-in. Linear-only	Redesigned
1	0	0	0	0	0	0.0	10915.0
2	0	0	0	0	1	17672.9	79899.5
3	0	0	0	1	0	63809.7	743.5
.	.	.	.	.	.	.	.
.	.	.	.	.	.	.	.
.	.	.	.	.	.	.	.
30	1	1	1	0	1	3200.8	68169.8
31	1	1	1	1	0	118857.7	0.0
32	1	1	1	1	1	19623.1	10370.0

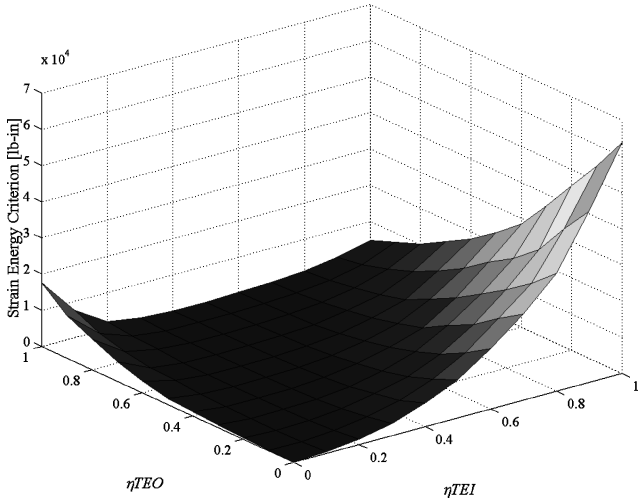

Fig. 8 Strain criterion vs η_{TEI} and η_{TEO}.

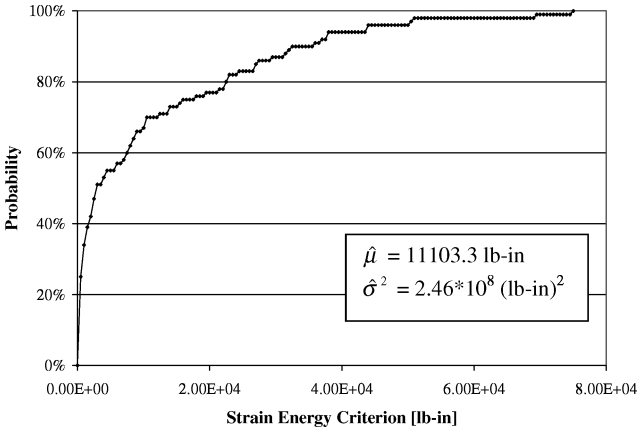

Fig. 9 CDF of strain energy criterion (100 samples).

in the strain energy criterion due to load variations, 100 samples, based on LHS, of the correction-load coefficient design space were analyzed. The results of this run are plotted as a CDF of the strain energy criterion in Fig. 9, with the mean and variance of the response sample shown. As evident from Fig. 9, no point sampled exceeded a strain energy criterion of approximately 75,000, well below the maximum value of 118,857.70 from Table 4. This provides some confidence that the most critical point has been selected.

Redesign of Structure with Most Critical Loads

A redesign to the rigid aerodynamic loads corresponding to case 31 of Table 4 was performed using the integrated AAW design process, by including the loads as an additional maneuver in the optimization. The starting point for this optimization was the final structural design of the integrated AAW design process with linear aerodynamics.

The final weight for the redesigned structure, along with the weight corresponding to the integrated AAW design with linear aerodynamics (linear only), is presented in Table 5. One notices about an 11% growth in weight for the redesigned structure.

Figure 10 presents a comparison of the total skin thickness of the upper wing surface between the linear-only integrated AAW optimization and the redesigned structure. The redesigned structure in most places is thicker than the linear-only structure, particularly near the root. This increase in material at the wing root is likely attributed to the reduction in the wing control surface deflections for the subsonic pull up with the critical loads. Because the control surface deflections are acting to provide load relief across the wing, and especially at the root, their smaller deflections, resulting from inclusion of the perturbed loads in the redesign, do not provide as much benefit as when they deflect to larger values in the linear-only case. Hence, this is the reason for the increased thickness at the wing root.

Table 6 shows the final control surface deflections and gear ratios for the subsonic pull up of the redesigned structure. They are compared to the final control surface deflections and gear ratios of the integrated approach based only on linear aerodynamics. The results in Table 6 are consistent with the additional load case to which the structure was redesigned. Because η_α, η_{LEI}, η_{LEO}, and $\eta_{\text{TEI}} = 1$ is the most critical case, one sees an increase in weight during the optimization, but also a reduction in the control surface deflections for the LEI, LEO, and TEI surfaces.

Next, the redesigned structure is evaluated on its ability to maintain strength requirements in the presence of load variations. This

Table 5 Final weights for linear-only and redesigned structure

Structure	Weight, lb
Redesigned	275.0
Linear only	248.0

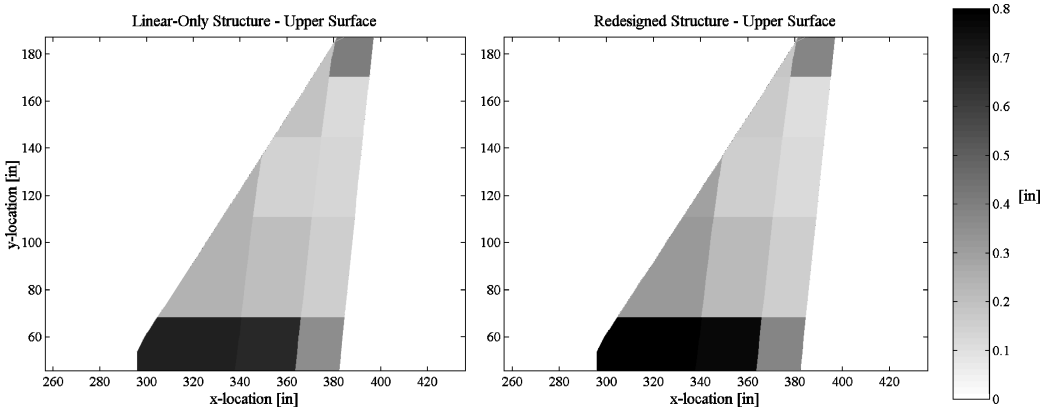

Fig. 10 Upper total Skin thickness (linear only vs redesign).

Table 6 Final control surface deflections and gear ratios of linear-only vs redesigned structures

Parameter	Redesigned	Linear only
δ_{LEI}, deg	−2.48	−11.52
δ_{LEO}, deg	−7.74	−30.00
δ_{TEI}, deg	9.72	29.86
δ_{TEO}, deg	−30.00	−30.00
δ_{HT}, deg	−6.92	2.05
α, deg	11.18	9.31
g_{LEI}	0.36	−5.64
g_{LEO}	1.12	−14.67
g_{TEI}	−1.40	14.60
g_{TEO}	4.33	−14.67

Table 7 Redesign of gear ratios for linear-only and redesigned structures

						Criterion, lb-in.	
Case	η_α	η_{LEI}	η_{LEO}	η_{TEI}	η_{TEO}	Linear-only	Redesigned
1	0	0	0	0	0	0.0	0.0
2	0	0	0	0	1	633.6	217.3
3	0	0	0	1	0	653.0	112.6
.	.	.	.	.	.	.	.
.	.	.	.	.	.	.	.
.	.	.	.	.	.	.	.
30	1	1	1	0	1	1360.1	5382.7
31	1	1	1	1	0	1733.9	0.0
32	1	1	1	1	1	247.5	0.0
Total						36107.6	16887.0

is done by evaluating the strain energy criterion for the redesigned structure, as was done for the linear-only structure, but with the reference strain energy vector $\{U\}^{\text{reference}}$ based on the perturbed loads to which the structure was redesigned (corresponding to $\eta_\alpha = \eta_{LEI} = \eta_{LEO} = \eta_{TEI} = 1$ and $\eta_{TEO} = 0$). In addition, the wing control surface deflections are fixed to their optimal values as found in the integrated AAW redesign.

Table 4 shows a comparison of the strain energy criterion at a select number of corner points of the correction-load coefficient design space for the original, linear-only structure and the redesigned structure. The characteristics of these new results show that when $\eta_{TEI} = 1$ and $\eta_{TEO} = 0$, the redesigned structure is vastly superior to the linear-only structure resulting in a significantly lower criterion value. However, when $\eta_{TEO} = 1$, then the redesigned structure generally has higher criterion values over the original one.

The higher strain energy criterion value of the redesigned structure as compared to the linear structure, for some correction-load coefficient values, is attributed to the inadequacy of the control surface deflections for these loading cases. The high-strain-energy criterion values for the redesigned structure when $\eta_{TEO} = 1$ indicate that the deflections that were found to be optimal when $\eta_{TEO} = 0$ are far from being optimal when $\eta_{TEO} = 1$, and the gearing ratios have to be redesigned.

Gear ratio redesign for each of the 32 loading cases of Table 4 was performed for both the redesigned structure and the linear-only structure, and the strain energy criterion of each case was evaluated. Selected results of this are presented in Table 7. For most all of the corner points, the redesigned structure has a much smaller criterion value than the linear-only structure. There are only a few cases for which the redesigned structure has a higher criterion value, whereas there are several cases for which the redesigned structure has no violation of strength constraints at all, resulting in a criterion value of zero. The results of Table 7 clearly show that the redesigned structure is more robust than the original structure. When the strain energy criterion for the cases of the linear-only structure and redesigned structure are each totaled, the redesigned structure has over a 50% lower strain energy criterion.

Table 7 also shows that even for the redesigned structure there are some loading conditions that do cause a violation of constraints and would require redesign if the structure is subject to them. Hence, the inclusion of only one most-critical case, although it produces a more robust design, does not result in a completely robust design, that is, one in which, for any loading condition, there are no violated constraints. To achieve a completely robust design, it is apparent that one would have to add more cases to the integrated AAW redesign. This can be done by either adding more corner points of the correction-load coefficient design space as additional maneuvers to the integrated AAW redesign (so that the structure is redesigned to more loading cases), or by designing each new redesigned structure to the new most-critical loading condition.

Conclusions

The study has presented a new methodology for aircraft structural design with consideration of inaccuracies in the aerodynamic maneuver load predictions. A statistical model for load inaccuracies due to the use of linear aerodynamic theory has been presented, in the form of correction loads, which represent typical differences between the actual loads and the loads predicted by linear theory. The load corrections were propagated to a strain energy criterion, which provides a measure of the amount of redesign that would be necessary when the structure is subject to variation in the loads to which it was designed. A sampling method was used to estimate the CDF of the strain energy criterion over the corrections-load coefficient design space, which provides a measure of the structure's robustness.

The method was applied to the design of an AAW concept, in which both the structural and control law designs are highly sensitive to inaccuracies in the maneuver loads. The most critical loading condition was identified and used to redesign the structure and control surface gear ratios. The redesigned structure was found to be 11% heavier, but significantly more robust than the original structure that was optimized to the linear loads only. The consideration of maneuver load corrections for an AAW with fixed gear ratios led to the discovery of an asymptote in the correction-load coefficient design space, in which certain loads, in combination with fixed gear ratios, led to catastrophic loading conditions. This phenomenon would not have been discovered had it not been for the consideration of inaccuracies in the loads. This discovery highlighted the need to redesign the gear ratios when the loads change.

The maneuver load-correction models developed in this study could also be used to augment the loads used in the large task of loads simulation of the general structural design process. This correction would then affect the identification of the most critical load cases and, subsequently, the sizing of the structure. In this way, because the structural design takes into account the inherent inaccuracies in loads due to linear aerodynamics, the structure should be more robust and, hence, result in a reduction in the number of design iterations.

References

[1]Miller, G. D., "Active Flexible Wing (AFW) Technology," U.S. Air Force Wright Aeronautical Labs, TR-87-3096, Wright–Patterson Air Force Base, Ohio, Feb. 1988.

[2]Pendleton, E. W., Bessette, D., Field, P. B., Miller, G. D., and Griffin, K. E., "Active Aeroelastic Wing Flight Research Program: Technical Program and Model Analytical Development," *Journal of Aircraft*, Vol. 37, No. 4, 2000, pp. 554–561.

[3]Miller, G. D., "An Active Flexible Wing Multi-Disciplinary Design Optimization Method," AIAA Paper 94-4412, Sept. 1994.

[4]Volk, J., and Ausman, J., "Integration of a Generic Flight Control System into ASTROS," AIAA Paper 96-1335, April 1996.

[5]Zillmer, S., "Integrated Multidisciplinary Optimization for Active Aeroelastic Wing Design," U.S. Air Force Wright Aeronautical Labs., Rept. WL-TR-97-3087, Wright–Patterson Air Force Base, Ohio, Aug. 1997.

[6]Love, M. H., Barker, D. K., Egle, D. D., Neill, D. J., and Kolonay, R. M., "Enhanced Maneuver Airloads Simulation for the Automated Structural Optimization System – ASTROS," AIAA Paper 97-1116, April 1997.

[7]Zink, P. S., Mavris, D. N., and Raveh, D. E., "Maneuver Trim Optimization Techniques for Active Aeroelastic Wings," *Journal of Aircraft*, Vol. 38, No. 6, 2001, pp. 1139–1146.

[8]Zink, P. S., Raveh, D. E., and Mavris, D. N., "Integrated Trim and Structural Design Process for Active Aeroelastic Wing Technology," *Journal of Aircraft*, Vol. 40, No. 3, 2003, pp. 523–531.

[9]Raveh, D. E., Karpel, M., and Yaniv, S., "Nonlinear Design Loads for Maneuvering Elastic Aircraft," *Journal of Aircraft*, Vol. 37, No. 2, 2000, pp. 313–318.
[10]Raveh, D. E., and Karpel, M., "Structural Optimization of Flight Vehicles with Computational-Fluid-Dynamics-Based Maneuver Loads," *Journal of Aircraft*, Vol. 36, No. 6, 1999, pp. 1007–1015.
[11]Johnson, E. H., and Venkayya, V. B., ASTROS Theoretical Manual, U.S. Air Force Wright Aeronautical Labs., Rept., AFWAL-TR-88-3028, Wright–Patterson Air Force Base, Ohio, Dec. 1988.
[12]Karpel, M., Moulin, B., and Love, M. H., "Modal-Based Structural Optimization with Static Aeroelastic and Stress Constraints," *Journal of Aircraft*, Vol. 34, No. 3, 1997, pp. 433–440.
[13]Karpel, M., "Modal-Based Enhancement of Integrated Design Optimization Schemes," *Journal of Aircraft*, Vol. 35, No. 3, 1998, pp. 437–444.
[14]Rodden, W. P., and Love, J. R., "Equations of Motion of Quasisteady Flight Vehicle Utilizing Restrained Static Aeroelastic Characteristics," *Journal of Aircraft*, Vol. 22, No. 9, 1995, pp. 802–809.
[15]McKay, M. D., Beckman, R. J., and Conover, W. J., "A Comparison of Three Methods for Selecting Values of Input Variables in the Analysis of Output from a Computer Code," *Technometrics*, Vol. 21, No. 2, 1979, pp. 239–245.
[16]Luo, X., and Grandhi, R. V., "ASTROS for Reliability-Based Multidisciplinary Structural Analysis and Optimization," AIAA Paper 95-1167, April 1995.
[17]Torng, T. Y., and Yang, R. J., "A Reliability-Based Design Optimization Procedure for Minimal Variations," AIAA Paper 94-1415, April 1994.
[18]Carmichael, R. L., Castellano, C. R., and Chen, C. F., "Analysis Methods in Aircraft Aerodynamics," NASA SP-228, Ames Research Center, Moffett Field, CA, Oct. 1969.
[19]Barker, D. K., and Love, M. H., "An ASTROS Application with Path Dependent Results," AIAA Paper 96-4139, Sept. 1996.
[20]Krist, S. L., Biedron, R. T., and Rumsey, C. L., *CFL3D User's Manual Version 5.0*, NASA TM-1998-208444, June 1998.
[21]Harder, R. L., and Desmarais, R. N., "Interpolation Using Surface Splines," *Journal of Aircraft*, Vol. 9, No. 2, 1972, pp. 189–191.